Comparisons of Initial Joint Angles and Test Buck Reaction Forces for Relaxed and Braced 5th Percentile Female and 50th Percentile Male Volunteers and Analogous Active Human Body Models in a Simulated Driver's Seat

Hana Chan, Karan S. Devane, Devon L. Albert, F. Scott Gayzik, and Andrew R. Kemper

Abstract The first objective of this study was to quantify the initial joint angles and reaction forces of relaxed and braced 5th percentile female and 50th percentile male volunteers in a rigid test buck to validate the alterations made to an existing test buck design. The second objective was to compare the volunteer data to analogous GHBMC models in order to determine if similar initial joint angles and reaction forces were achieved in silico. Six female and six male volunteers experienced low-speed sled tests in relaxed and braced conditions in a rigid test buck, instrumented with load cells at each subject-test buck interface. The test buck, originally designed for 50th percentile males, was modified with spacers for 5th percentile females to obtain similar initial joint angles between sexes. Matched simulations were performed using the GHBMC F05-OS+Active and M50-OS+Active models. The initial positions and force distributions of the female volunteers were very similar to those of the male volunteers for each respective muscle condition, indicating that the test buck design successfully achieved similar initial conditions between sexes. The volunteers and models also had similar initial positions and force distributions when relaxed, with some observed differences when braced. Overall, the results suggest that the models are generally capable of capturing the initial conditions observed in the volunteers for both muscle conditions.

Keywords Computational model, force distribution, initial conditions, initial position, validation.

I. INTRODUCTION

Computational human body models (HBMs) that incorporate active musculature can be used to better understand and predict occupant response and injury risk during pre-crash events and subsequent frontal motor vehicle collisions (MVCs) [1-5]. In order for these models to accurately represent the response of live occupants, they must be validated with appropriate volunteer data. This includes validating the models with volunteer data that represent a wide range of occupant populations, including 5th percentile females. However, in order to make direct comparisons between the occupant responses of small female volunteers and other demographic groups, such as the typically studied 50th percentile male, the initial conditions must be the same for all subjects in an experimental scenario. This is essential to ensure that any observed differences in occupant response are not caused by discrepancies in initial positioning. It is well established that similar initial conditions between subject groups is highly important for generating matched data sets for comparison [6-9].

Establishing similar initial conditions between computational HBMs and validation data (either from volunteer or post-mortem human surrogate (PMHS) studies) is also necessary for generating simulations that are directly comparable. Most HBM validation efforts have focused on matching the model's response to the response of volunteers or PMHS during dynamic full-body sled tests that simulate both pre-crash and crash events [1, 2, 4, 5, 10-14]. Less of the research literature has focused specifically on matching the initial conditions, or investigating the effect of discrepancies in initial positioning, between HBMs and validation data prior to the start of these tests, on the subsequent dynamic response [10, 12]. However, capturing the initial conditions of occupants in HBMs should be carefully considered during model development as changes in initial positioning can potentially affect occupant response and injury risk during the pre-crash and crash phases of frontal MVCs [15-18]. A few previous studies have investigated the mass distribution of the GHBMC 50th percentile male occupant model, but

A. R. Kemper (phone: +1 540 231 2465, email: akemper@vt.edu) is an Associate Professor, H. Chan is a PhD student, and D. L. Albert is a Research Assistant Professor of Biomedical Engineering in the Center for Injury Biomechanics at Virginia Tech in Blacksburg, VA, USA. K. S. Devane is a PhD student and F. S. Gayzik is an Associate Professor of Biomedical Engineering in the Center for Injury Biomechanics at the Wake Forest University School of Medicine in Winston-Salem, NC, USA.

these studies focused on quantifying individual body segment masses and centres of gravity as opposed to reaction forces at the interface between the occupants and test buck [19, 20]. Additionally, it is also important to create similar initial conditions when comparing between subject groups as factors such as occupant mass, stature, posture, and bracing level have been shown to significantly affect injury risk in frontal MVCs [21].

A recent human volunteer sled testing study was conducted on twelve volunteers (six female and six male) to quantify the kinematics, kinetics, and muscle activity of 5th percentile female and 50th percentile male occupants in response to 1 g and 2.5 g sled pulses that simulated autonomous braking events and low-severity frontal MVCs, respectively [22]. Sled testing was conducted using a custom rigid test buck. For the 5th percentile female volunteers, the test buck was modified to accommodate their smaller anthropometry. The data and analyses from this sled testing study will be used to compare occupant responses between 5th percentile female and 50th percentile male volunteers, as well as further develop and validate the GHBMC 5th percentile female and 50th percentile male simplified occupant models with active musculature. To ensure that the test buck alterations created similar initial conditions between the female and male volunteers and that the model responses from matched simulations accurately represented the response of analogous volunteers, a separate analysis was required to compare the initial conditions between the volunteer demographic groups, as well as the volunteers and models.

The objectives of the analysis presented here were twofold. The first objective was to quantify the initial joint angles and reaction forces of relaxed and braced 5th percentile female and 50th percentile male volunteers in a rigid test buck to validate the alterations made to the test buck design to accommodate the anthropometry of 5th percentile females. The second objective was to compare the volunteer data to analogous GHBMC models to determine if similar initial joint angles and test buck reaction forces were achieved.

II. METHODS

Experimental Testing

Six female volunteers and six male volunteers participated in this study (Table I). The female and male volunteers were approximately 5th percentile and 50th percentile height and weight, respectively, according to [23]. All human volunteer testing was approved by the Virginia Tech Institutional Review Board. Each volunteer signed an informed consent form before participating in the study at the start of each test day.

TABLE I

VOLUNTEER AND MODEL DEMOGRAPHICS AND ANTHROPOMETRY (AVERAGE ± STANDARD DEVIATION)

Sex	Age (years)	Height (cm)	Weight (kg)
Female Volunteer	24.0 ± 2.8	156.6 ± 5.9	50.0 ± 2.4
Female Model (GHBMC F5-OS)	24	149.9	54.1
Male Volunteer	23.3 ± 2.0	175.9 ± 2.1	76.1 ± 3.5
Male Model (GHBMC M50-OS)	26	174.9	78.4

The analysis presented here is part of a larger study where each volunteer was exposed to multiple low-speed sled tests on two separate test days spaced 7-10 days apart [22]. On a given test day, volunteers experienced either purely frontal (principal direction of force (PDOF) = 0°) or frontal-oblique (PDOF = 30°) sled tests. On each test day, volunteers experienced four sled tests, consisting of two pulse severities and two muscle conditions per pulse severity, in the following order: 1 g (Δv = 9.47 ± 0.25 kph) relaxed, 1 g braced, 2.5 g (Δv = 5.33 ± 0.27 kph) relaxed, and 2.5 g braced. The pulse severities were chosen to simulate an autonomous braking event (1 g) and a low severity frontal MVC (2.5 g) [22]. The dynamic data from these tests are not included in this analysis. Only the static data collected before the start of the sled pulse during each test were included.

All sled tests were performed on a custom rigid test buck and mini-sled accelerated by a pneumatic piston [24]. The test buck was instrumented with reaction load cells at each subject-test buck interface (Fig. 1). Six-axis load cells were installed at the left foot pedal (Denton-1716A, 13.3 kN, Rochester Hills, MI, USA), right foot pedal (Denton-1794A, 13.3 kN), and seat pan and seat back (Denton-2513, 44 kN) (Fig. 1). A five-axis load cell was installed at the steering column (Denton-1968, 22.2 kN) (Fig. 1). The test buck, originally designed for 50th

percentile male volunteers, was modified for the 5th percentile female volunters in order to obtain similar initial joint angles for both sexes. Rigid aluminum spacers were installed between the test buck frame and reaction load cells at each interface to position the reaction surfaces in locations that would accommodate the anthropometry of a 5th percentile female and maintain consistent resting joint angles with 50th percentile male volunteers from a previous study that used the same test buck to test volunteers in low-speed sled tests (Fig. 1, Table II) [24]. Dimensions for the spacers (thicknesses in particular) were determined using two females of approximately 5th percentile female anthropometry from the research group. Resting joint angle measurements were recorded using a goniometer while the researchers took turns sitting in the test buck in a manner similar to the volunteers prior to the test start. As incremental height adjustments to placeholder spacers were made, the researchers' joint angles were measured. After the spacer dimensions were selected such that the reseachers' resting joint angles matched those of the 50th percentile male volunteers from the previous study as closely as possible [24], the final spacer dimensions were confirmed by measuring the resting joint angles (using a goniometer) of a 5th percentile female Hybrid III anthropomorphic test device (HIII ATD) seated in the test buck. The D-ring location for female volunteers in the current study was also adjusted to be 7.62-10.16 cm lower than the location used for male volunteers. This location was also chosen by confirming a reasonable and comfortable belt path of the two female researchers and the 5th percentile female HIII ATD. Specific test buck dimensions for both the 50th percentile male and 5th percentile female anthropometries are located in the appendix (Fig. A6-A7).

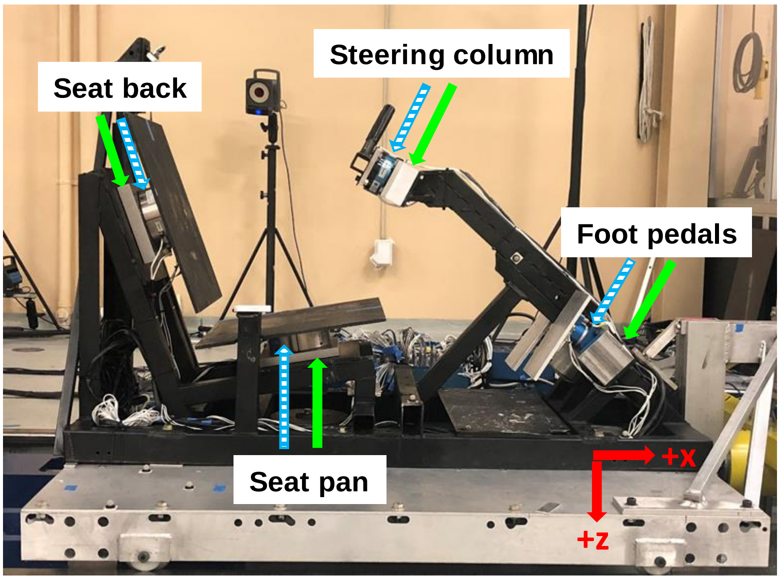

Fig. 1. Custom rigid test buck and mini-sled instrumented with reaction load cells (striped blue arrows), which has been modified for 5th percentile female volunteers with rigid aluminum spacers (green arrows) at each subject-test buck interface.

TABLE II

TEST BUCK INTERFACE ANGLES AND SPACER THICKNESSES

Interface	Angle (°) *	Spacer Thickness (cm)
Seat Back	70	3.18
Seat Pan	10	2.22
Steering Column	65	4.40
Left Foot Pedal	55	10.96
Right Foot Pedal	58	10.00

* acute angles measured from the horizontal plane

Before each sled test, subjects were positioned in the centre of the test buck (mediolaterally) with their feet centred on the foot pedals (without additional vertical support) and their hands on the rigid steering wheel handles. For the relaxed tests, subjects were instructed to sit in a relaxed manner, face forward, and watch a monitor playing a show or movie (Fig. 2). They were told that the pulse would be triggered randomly in the next few minutes. When the subjects appeared relaxed, relatively still, and focused on the monitor for at least one minute, the pulse was triggered using a switch that was out of sight from the subjects so they were unaware of the test start. For the braced tests, subjects were also instructed to sit in a relaxed manner and face forward at first, in a similar manner to the relaxed tests. A countdown was used to instruct subjects when to begin bracing (two seconds prior to the test start) and when the test would begin. Subjects were instructed to brace as if they were anticipating a crash event. Specifically, they were told to push with maximum effort on the steering wheel and foot pedals with their upper and lower extremities, respectively, and the seat back with their torso (Fig. 3). A standard 3 kN load-limiting United States driver-side three-point seatbelt from a Toyota Camry that fits model years 2007-2011 was used for all sled tests. The slack in the seatbelt was removed manually by the researchers a few minutes prior to the start of each sled test, while monitoring the belt loads in real time.

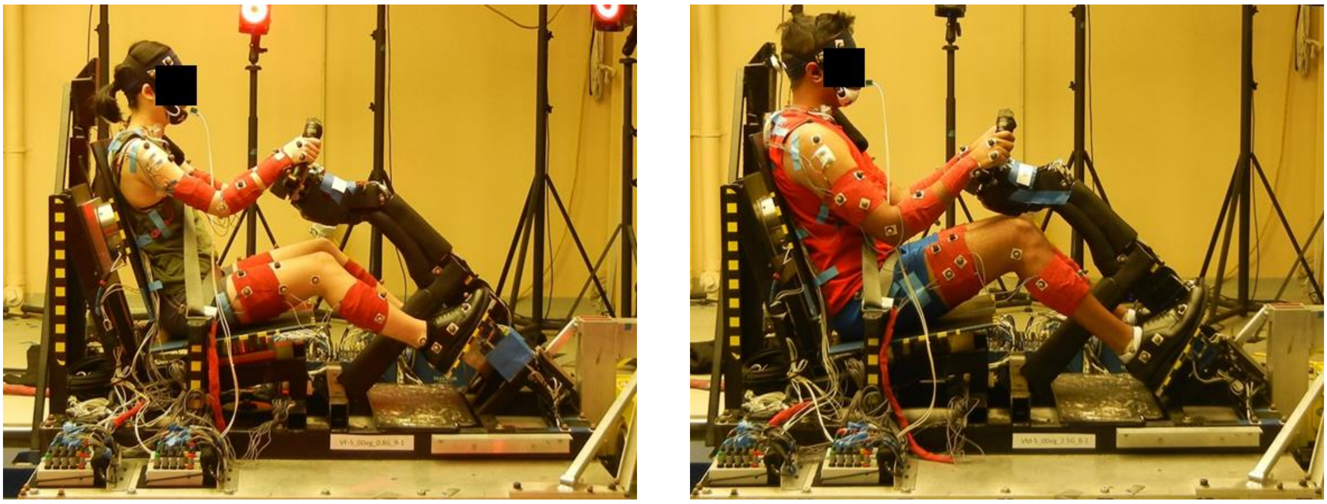

Fig. 2. Female (left) and male (right) subjects seated in the test buck prior to the start of a relaxed test.

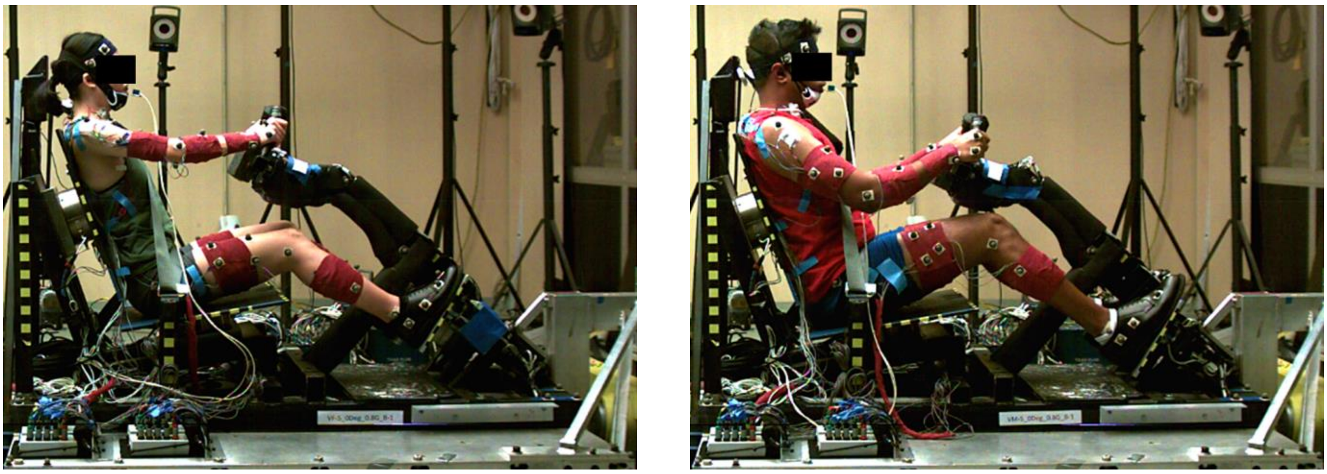

Fig. 3. Female (left) and male (right) subjects seated in the test buck prior to the start of a braced test.

A Vicon MX motion capture system (Vicon Motion Systems, Oxford, United Kingdom) was used to quantify the locations (3D coordinates) of the subjects and the test buck (1000 Hz sampling rate) prior to and during each sled test. Retro-reflective markers were attached to the test buck and subjects using a custom marker set that included key anatomical locations and ancillary segment markers (Fig. 2-3). Specific regions of interest included the centre of gravity of the head (head CG), seventh cervical vertebra (C7), shoulders, elbows, hips, and knees (Table III). Certain markers, e.g., left acromion, left and right greater trochanter, were removed from some subjects prior to sled tests to prevent contact between the markers and the shoulder and lap belts, and some markers were obstructed from the field of view during some subjects' sled tests. These missing markers were reconstructed using static capture data collected prior to sled testing and rigid body mechanics [24].

An onboard data acquisition system (DTS TDAS Pro, Seal Beach, CA, USA) was used to record reaction load data (20 kHz). Data were recorded for three seconds pre-trigger and three seconds post-trigger for each sled test. For the relaxed tests, data were collected during the relaxed pre-trigger state (3 seconds) and the test event (3 seconds). For the braced tests, data were collected during the relaxed pre-trigger state (1 second), the pre-impact bracing state (2 seconds), and the test event (3 seconds). Empty test buck static data were also collected at least once per test day (either before testing, after testing, or both). The data from each sled test were time-shifted so that the initiation of the sled pulse occurred at 180 ms (test start) for each test.

TABLE III
MARKERS USED TO REPRESENT ANATOMICAL LOCATIONS

Region of Interest	Location of Marker(s)
Head CG	Average of left and right head CG *
C7	Directly above C7 spinous process
Shoulders	Left and right acromia
Elbows	Left and right lateral humeral epicondyles
Wrists	Left and right radial styloid processes
Hips	Left and right greater trochanters
Knees	Left and right lateral femoral epicondyles
Ankles	Left and right lateral malleoli
Toes	Left and right averages of 1^{st} and 4^{th} metatarsals

* The location of the head CG was calculated as the average position of markers placed on a headband as close as possible to the left and right anterior-superior insertion points of the helices of the ears [25, 26]

Computational Modelling

Matched simulations were performed using the GHBMC 5^{th} percentile female (F05-OS+Active) and 50^{th} percentile male (M50-OS+Active) simplified occupant models with active musculature (Fig. 4). Both models were gravity settled, repositioned in a driving posture, and belted in the test buck as per the procedure detailed in [1]. The models were repositioned to match the volunteers' initial postures closely. After repositioning and belting, the models were simulated again to remove any residual motion in the downward (positive Z) direction and remove any slack in the seatbelt. The slack in the seatbelt was removed by using an 18 N initial tension value for the retractor loading curve. Both the relaxed and braced models used a closed-loop feedback control system to calculate muscle activation for each muscle. This control system utilized joint angles as the control variables. For the braced simulations, muscle activation was applied to obtain initial braced postures by setting the target joint angles to be greater than the initial relaxed posture joint angles so that the model braced itself against the test buck surfaces [1]. No muscle activation was applied for the relaxed simulations. Initial joint angles and reaction forces for the relaxed and braced conditions were extracted at 110 and 210 ms, respectively.

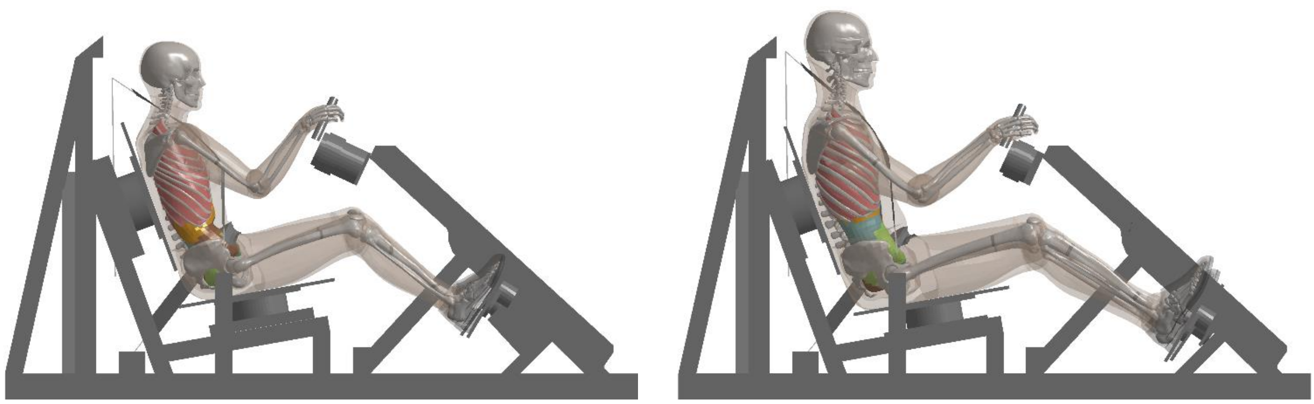

Fig. 4. F05-OS+Active (left) and M50-OS+Active (right) simplified occupant models at the test start.

Joint Angles

Initial joint angles at the test start were quantified for the volunteers using the 3D locations of motion capture markers at the time immediately preceding the beginning of sled motion (180 ms). Joint angles were limited to the sagittal plane, i.e., only X and Z positions were considered, and were calculated as the included angle defined by three motion capture markers using the Law of Cosines. Neck, shoulder, hip, knee, and ankle joint angles were calculated using the anatomical locations described in Fig. 5 and Table IV, and were calculated bilaterally for the shoulders, elbows, hips, knees, and ankles. Joint angles were calculated for all tests for each subject and were grouped according to muscle condition. The joint angles were averaged across tests for each subject and then across all subjects within each muscle condition and each sex, to produce average female and male joint angles for the relaxed and braced conditions. Joint angles were quantified using the same methodology for the relaxed and braced female and male models using analogous anatomical locations and calculations. Initial joint angles at the test start were compared between sexes, muscle conditions, and the volunteers and models (Eq. 1-3, respectively), and reported as signed differences.

$$\Delta\theta_{M-F} = \theta_{male} - \theta_{female} \tag{1}$$

$$\Delta\theta_{B-R} = \theta_{braced} - \theta_{relaxed} \tag{2}$$

$$\Delta\theta_{Mod-Vol} = \theta_{model} - \theta_{volunteer} \tag{3}$$

TABLE IV
ANATOMICAL LOCATIONS USED TO CALCULATE JOINT ANGLES

Joint Angle	Vertex Point(s)	Endpoint(s)	Endpoint(s)
Neck	C7	Head CG	Average of left and right hips
Shoulder	Shoulder	Elbow	Hip
Elbow	Elbow	Shoulder	Wrist
Hip	Hip	C7	Knee
Knee	Knee	Hip	Ankle
Ankle	Ankle	Knee	Toe

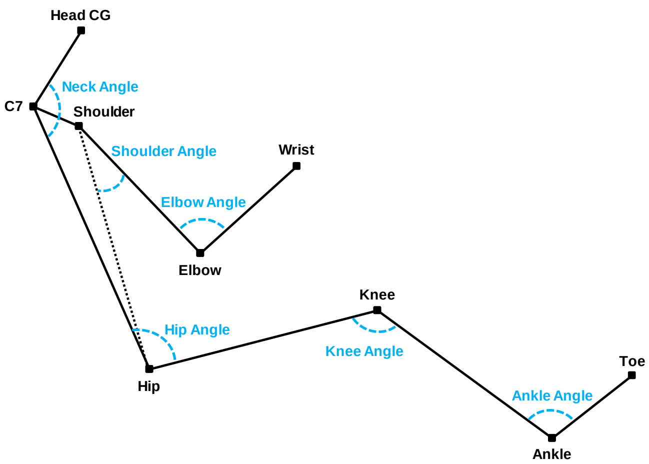

Fig. 5. Included joint angles (blue) and anatomical locations (black) used to calculate joint angles.

Reaction Forces

Initial reaction forces were quantified for the volunteers using the load cell data during pre-trigger, or prior to the test start. For the relaxed condition, pre-trigger load cell data were averaged over the pre-trigger time when subjects were in a relaxed state, from a combination of relaxed and braced tests from both test days. For the braced condition, pre-trigger load cell data from braced tests (from both test days) were recorded when subjects were at the end of their pre-impact bracing state, i.e., at the time immediately preceding the beginning of sled motion (180 ms). To quantify the reaction forces, the empty test buck static forces were subtracted from the forces recorded before sled motion for each test. This removed any offsets from the load cells that were due to the weight of the sled components, isolating the reaction forces exerted by the subjects. The resulting reaction forces were filtered using SAE Channel Frequency Class (CFC) 60 Hz, compensated for crosstalk, and converted to the SAE J211 coordinate system [27].

For each sled test, the individual horizontal and vertical force components were calculated for each load cell's X and Z channels, and each load cell surface, using trigonometry (Fig. 6). For each load cell surface, the vertical force components from the X and Z channels were summed to generate an overall vertical reaction force for the surface (Fig. 6, Eq. 4). Similarly, the horizontal force components from the X and Z channels were summed to generate an overall horizontal reaction force for each load cell surface (Fig. 6, Eq. 5). Then, the vertical reaction forces from all the load cell surfaces were summed together to calculate each subject's total weight (Eq. 6). The percent vertical and horizontal force distributions for each load cell surface were calculated as the vertical and horizontal reaction forces, respectively, on each load cell surface divided by the total subject weight (Eq. 7-8). The resultant reaction forces for each load cell surface (except for the seat pan) were also calculated using each load cell's X, Y, and Z channels (Eq. 9). Data from the seat pan's Y channel was not available for all volunteers, so it was not included in the resultant reaction force calculations for all volunteers and models for consistency. For volunteers where the seat pan's Y channel was available, differences between the X-Y-Z and X-Z resultant reaction force calculations were negligible. The percent resultant force distributions for each load cell surface were calculated as the resultant reaction force divided by the total subject weight (Eq. 10).

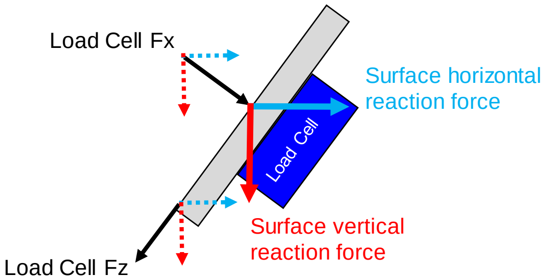

Fig. 6. Horizontal (blue) and vertical (red) force components for a foot pedal load cell's X and Z channels (dashed) and the overall load cell surface (solid).

$$Surface\ vertical\ reaction\ force = LC\ Fx_{vertical} + LC\ Fz_{vertical} \tag{4}$$

$$Surface\ horizontal\ reaction\ force = LC\ Fx_{horizontal} + LC\ Fz_{horizontal} \tag{5}$$

$$Total\ subject\ weight = \sum Vertical\ reaction\ forces\ from\ all\ surfaces \tag{6}$$

$$\%\ Vertical\ force\ distribution = \frac{Surface\ vertical\ reaction\ force}{Total\ subject\ weight} \tag{7}$$

$$\%\ Horizontal\ force\ distribution = \frac{Surface\ horizontal\ reaction\ force}{Total\ subject\ weight} \tag{8}$$

$$Surface\ resultant\ reaction\ force = \sqrt{(LC\ Fx)^2 + (LC\ Fy)^2 + (LC\ Fz)^2} \tag{9}$$

$$\%\ Resultant\ force\ distribution = \frac{Surface\ resultant\ reaction\ force}{Total\ subject\ weight} \tag{10}$$

The percent force distributions (vertical, horizontal, and resultant) were calculated for all tests for each subject and were grouped according to muscle condition. The force distributions were averaged across tests for each subject and then across all subjects within each muscle condition and each sex, to produce average female and male force distributions for the relaxed and braced conditions. Reaction forces and percent force distributions (vertical, horizontal, and resultant) were quantified using the same methodology for the relaxed and braced female and male models using analogous calculations. Vertical (VΔ%), horizontal (HΔ%), and resultant (RΔ%) percent force distributions at the test start were compared between sexes, muscle conditions, and the volunteers and models (Eq. 11-13, respectively), and reported as signed differences.

$$\Delta\%_{M-F} = \%_{male} - \%_{female} \tag{11}$$

$$\Delta\%_{B-R} = \%_{braced} - \%_{relaxed} \tag{12}$$

$$\Delta\%_{Mod-Vol} = \%_{model} - \%_{volunteer} \tag{13}$$

III. RESULTS

Comparisons of initial joint angles and vertical, horizontal, and resultant percent force distributions between sexes, muscle conditions, and the volunteer and models are reported below as signed differences.

Joint Angles

The female and male volunteers generally had similar joint angles for both the relaxed and braced conditions ($\Delta\theta_{M\text{-}F}$ = -9° to 5°), except for minimal differences in the braced left elbow angle ($\Delta\theta_{M\text{-}F,\ left\ elbow}$ = -13°) (Fig. 7, Table V, Fig. A1, Table AI). The female and male models also generally had similar joint angles for each respective muscle condition ($\Delta\theta_{M\text{-}F}$ = -4° to 8°), except for differences in the neck, elbow, and left knee angles ($\Delta\theta_{M\text{-}F,\ neck}$ = 10° to 19°, $\Delta\theta_{M\text{-}F,\ elbow}$ = 15° to 25°, $\Delta\theta_{M\text{-}F,\ left\ knee}$ = 15°).

Bracing increased the joint angles of nearly all body regions for both the volunteers and models ($\Delta\theta_{B\text{-}R}$ = 2° to 13°), particularly the elbows ($\Delta\theta_{B\text{-}R,\ elbow}$ = 17° to 32°) (Fig. 8, Table V, Fig. A2, Table AII). Bracing did not affect the neck angle for the female volunteers ($\Delta\theta_{B\text{-}R,\ neck}$ = 0°).

Minimal differences in joint angles were generally observed between the volunteers and models for both sexes and muscle conditions ($\Delta\theta_{Mod\text{-}Vol}$ = -10° to 9°), except for select locations (Fig. 9, Table V, Fig. A3, Table AIII). Differences were observed in the elbow angle between the volunteers and models for the males when relaxed and braced ($\Delta\theta_{Mod\text{-}Vol,\ elbow}$ = 16° to 18°) and the females when braced ($\Delta\theta_{Mod\text{-}Vol,\ elbow}$ = -22° to -16°). Differences were also observed in the neck and left knee angles between the male volunteers and models when braced ($\Delta\theta_{Mod\text{-}Vol,\ neck}$ = 15°, $\Delta\theta_{Mod\text{-}Vol,\ left\ knee}$ = 11°).

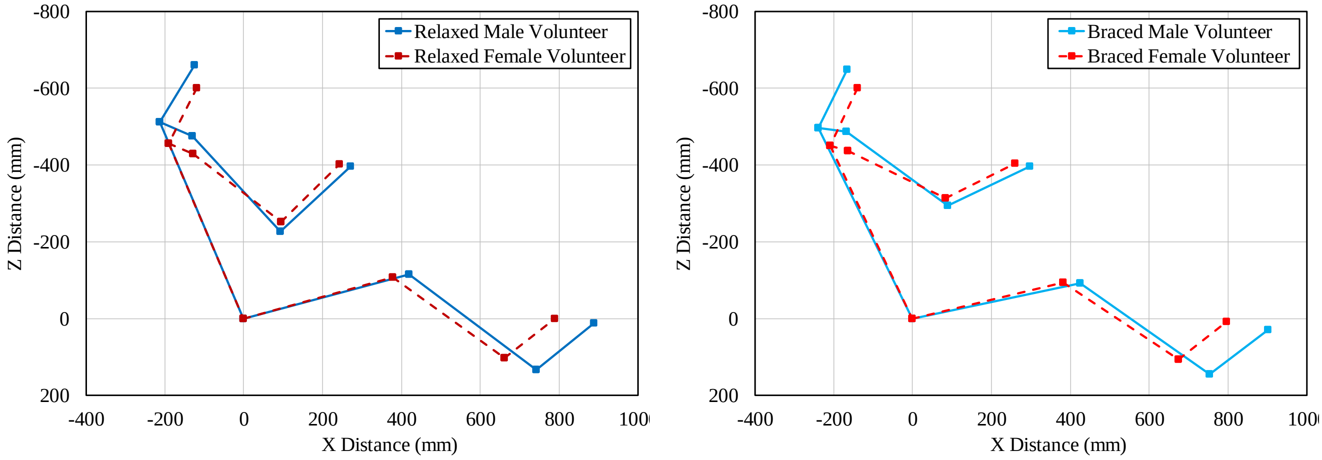

Fig. 7. Average initial positions of the male (blue) and female (red) volunteers for the relaxed (left) and braced (right) conditions. Marker positions are aligned at the hip.

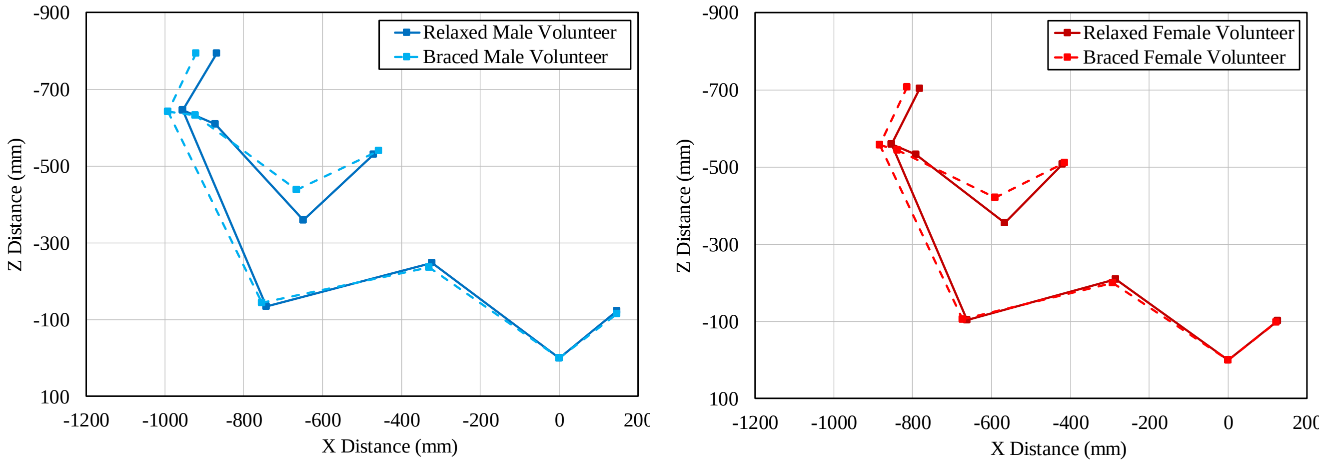

Fig. 8. Average initial positions of the male (left) and female (right) volunteers for the relaxed (solid) and braced (dashed) conditions. Marker positions are aligned at the ankle.

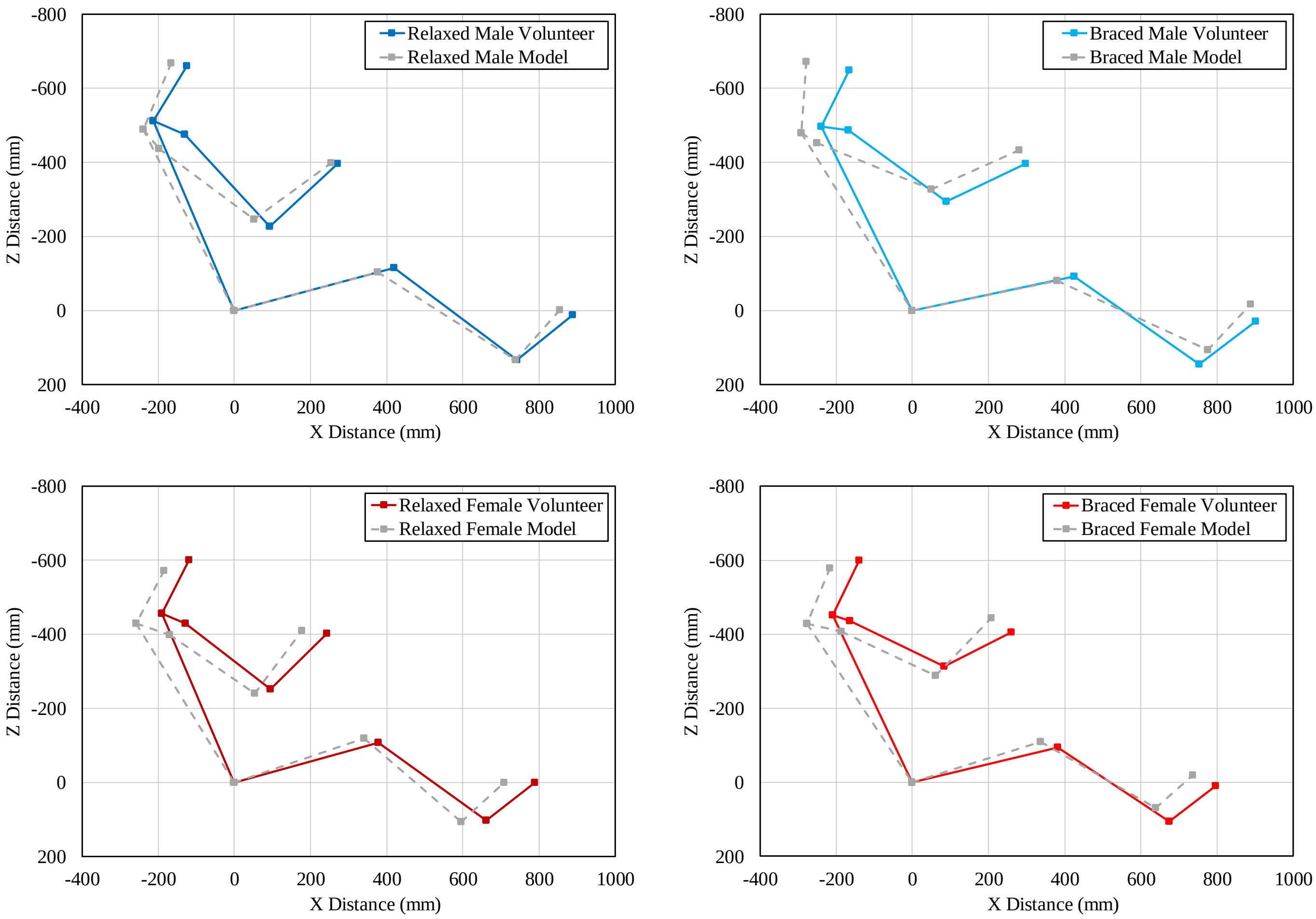

Fig. 9. Average initial positions of the male volunteers and male models (top), and the female volunteers and female models (bottom), for the relaxed (left) and braced (right) conditions. Marker positions are aligned at the hip.

TABLE V

VOLUNTEER AND MODEL JOINT ANGLES (°) (AVERAGE ± STANDARD DEVIATION)

	Relaxed				*Braced*			
	Female		Male		Female		Male	
	Volunteer	Model	Volunteer	Model	Volunteer	Model	Volunteer	Model
Neck	130.9 ± 4.4	121.8	126.9 ± 4.7	131.9	130.8 ± 4.2	125.4	129.6 ± 7.5	144.7
Left shoulder	36.4 ± 4.6	31.8	28.0 ± 3.6	28.5	44.6 ± 7.0	39.8	35.5 ± 4.2	38.3
Right shoulder	33.8 ± 4.8	31.5	25.6 ± 3.8	28.4	41.1 ± 5.5	39.8	33.0 ± 4.6	38.1
Left elbow	97.8 ± 8.2	91.1	89.2 ± 8.4	106.5	130.3 ± 15.8	108.0	117.4 ± 15.2	132.9
Right elbow	95.0 ± 9.3	90.5	87.5 ± 9.4	105.7	122.9 ± 13.6	107.2	117.0 ± 19.7	132.6
Left hip	96.0 ± 6.5	100.5	97.6 ± 4.2	102.6	100.2 ± 6.4	103.6	104.0 ± 5.4	111.8
Right hip	98.5 ± 6.9	103.3	97.0 ± 3.5	98.9	102.2 ± 7.3	106.4	103.0 ± 5.5	106.7
Left knee	125.6 ± 9.5	117.8	129.1 ± 6.4	133.0	129.5 ± 10.1	130.3	134.2 ± 8.2	145.7
Right knee	130.9 ± 10.9	121.5	125.1 ± 6.7	130.1	134.7 ± 9.5	133.0	130.2 ± 9.8	139.6
Left ankle	104.9 ± 5.4	96.7	104.7 ± 3.9	100.4	106.5 ± 5.3	109.3	108.1 ± 5.3	109.7
Right ankle	104.8 ± 5.8	94.9	100.4 ± 5.1	94.8	107.3 ± 5.2	106.3	104.4 ± 6.7	104.5

Force Distributions

The volunteers and models had similar vertical force distributions between females and males for each respective muscle condition on all the reaction surfaces (V$\Delta\%_{M\text{-}F}$ = -5% to 6%) (Fig. 10-11, Table VI-VII, Table AIV-AV, Table AX). The volunteers and models also generally had similar horizontal and resultant force distributions between females and males for each respective muscle condition (H$\Delta\%_{M\text{-}F}$ = -8% to 4%, R$\Delta\%_{M\text{-}F}$ = -9% to 4%) (Fig.

10-11, Table VIII-XI, Fig. A4-A5, Table AVI-AIX, Table AXI-AXII). Minimal differences in horizontal and resultant force distributions were observed between the females and males on the right foot and steering column for the braced volunteers ($H\Delta\%_{\text{M-F, right foot}}$ = -10%, $H\Delta\%_{\text{M-F, column}}$ = 13%, $R\Delta\%_{\text{M-F, right foot}}$ = -12%, $R\Delta\%_{\text{M-F, column}}$ = 14%), and on the right foot and seat back for the braced models ($H\Delta\%_{\text{M-F, right foot}}$ = -18%, $H\Delta\%_{\text{M-F, seat back}}$ = 13%, $R\Delta\%_{\text{M-F, right foot}}$ = -18%, $R\Delta\%_{\text{M-F, column}}$ = -11%).

Bracing increased the vertical force distributions for the volunteers and models on the foot pedals and seat back ($V\Delta\%_{\text{B-R, foot}}$ = 5% to 15%, $V\Delta\%_{\text{B-R, back}}$ = 15% to 31%), and decreased the vertical force distribution on the seat pan ($V\Delta\%_{\text{B-R, pan}}$ = -46% to -34%) (Fig. 10-11, Table VI-VII, Table AIV-AV, Table AXIII). Bracing did not affect the vertical force distribution on the steering column for the volunteers and models ($V\Delta\%_{\text{B-R, column}}$ = -1% to 1%). Compared to the vertical force distributions, bracing had a larger increasing effect on the horizontal force distributions for the volunteers and models on the foot pedals and seat back ($H\Delta\%_{\text{B-R, foot}}$ = 29% to 54%, $H\Delta\%_{\text{B-R, back}}$ = -111% to -86%, note: the horizontal force on the seat back became more negative due to bracing) (Fig. 10-11, Table VIII-IX, Table AVI-AVII, Table AXIV). However, bracing had a smaller decreasing effect on the volunteers' and models' horizontal force distribution, compared to the vertical force distribution, for the seat pan ($H\Delta\%_{\text{B-R, pan}}$ = -8% to -16%). In contrast to the negligible effect bracing had on the volunteers' and models' steering column vertical force distribution, bracing increased the steering column horizontal force distribution (models: $H\Delta\%_{\text{B-R, column}}$ = 22% to 23%, volunteers: $H\Delta\%_{\text{B-R, column}}$ = 41% to 52%). Bracing also increased the resultant force distributions for the volunteers and models on the foot pedals, steering column, and seat back ($R\Delta\%_{\text{B-R, foot}}$ = 30% to 55%, models: $R\Delta\%_{\text{B-R, column}}$ = 8% to 10%, $R\Delta\%_{\text{B-R, back}}$ = 86% to 97%; volunteers: $R\Delta\%_{\text{B-R, column}}$ = 35% to 50%, $R\Delta\%_{\text{B-R, back}}$ = 118% to 124%) (Table X-XI, Fig. A4-A5, Table AVIII-AIX, Table AXV). The resultant force distribution for the volunteers and models on the seat pan decreased due to bracing ($R\Delta\%_{\text{B-R, pan}}$ = -45% to -36%).

Minimal differences in vertical force distributions were observed between the volunteers and models for both sexes and muscle conditions on all the reaction surfaces ($V\Delta\%_{\text{Mod-Vol}}$ = -11% to 12%) (Fig. 10-11, Table VI-VII, Table AIV-AV, Table AXVI). The observed horizontal force distributions between the volunteers and models were generally similar for both sexes and muscle conditions ($H\Delta\%_{\text{Mod-Vol}}$ = -8% to 7%), except on the steering column and seat back when braced ($H\Delta\%_{\text{Mod-Vol, column}}$ = -34% to -22%, $H\Delta\%_{\text{Mod-Vol, back}}$ = 16% to 31%) (Fig. 10-11, Table VIII-IX, Table AVI-AVII, Table AXVII). The resultant force distributions were similar for both sexes between the volunteers and models on the foot pedals and seat pan when braced ($R\Delta\%_{\text{Mod-Vol, foot}}$ = -7% to 4%, $R\Delta\%_{\text{Mod-Vol, pan}}$ = 7% to 11%), and on all the reaction surfaces when relaxed ($R\Delta\%_{\text{Mod-Vol}}$ = -9% to 4%) (Table X-XI, Fig. A4-A5, Table AVIII-AIX, Table AXVIII). As observed with the horizontal resultant force distributions, differences in resultant force distributions between the volunteers and models were also observed on the steering column and seat back when braced ($R\Delta\%_{\text{Mod-Vol, column}}$ = -37% to -24%, $R\Delta\%_{\text{Mod-Vol, back}}$ = -42 to -27%).

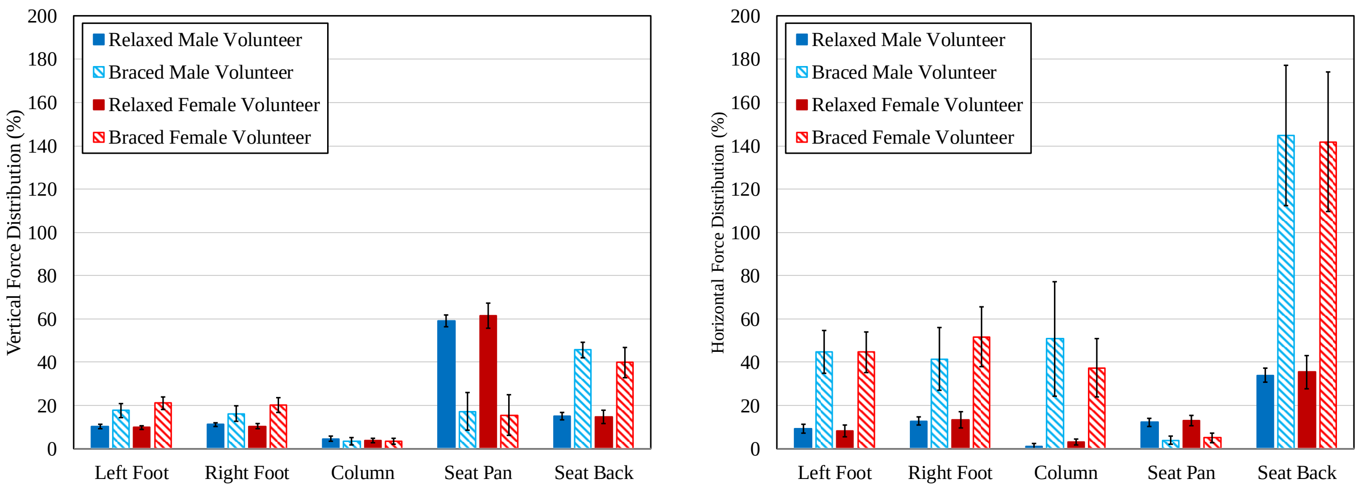

Fig. 10. Average vertical (left) and horizontal (right) force distributions for the male (blue) and female (red) volunteers for the relaxed (solid) and braced (striped) conditions. All percent force distributions are reported as absolute values.

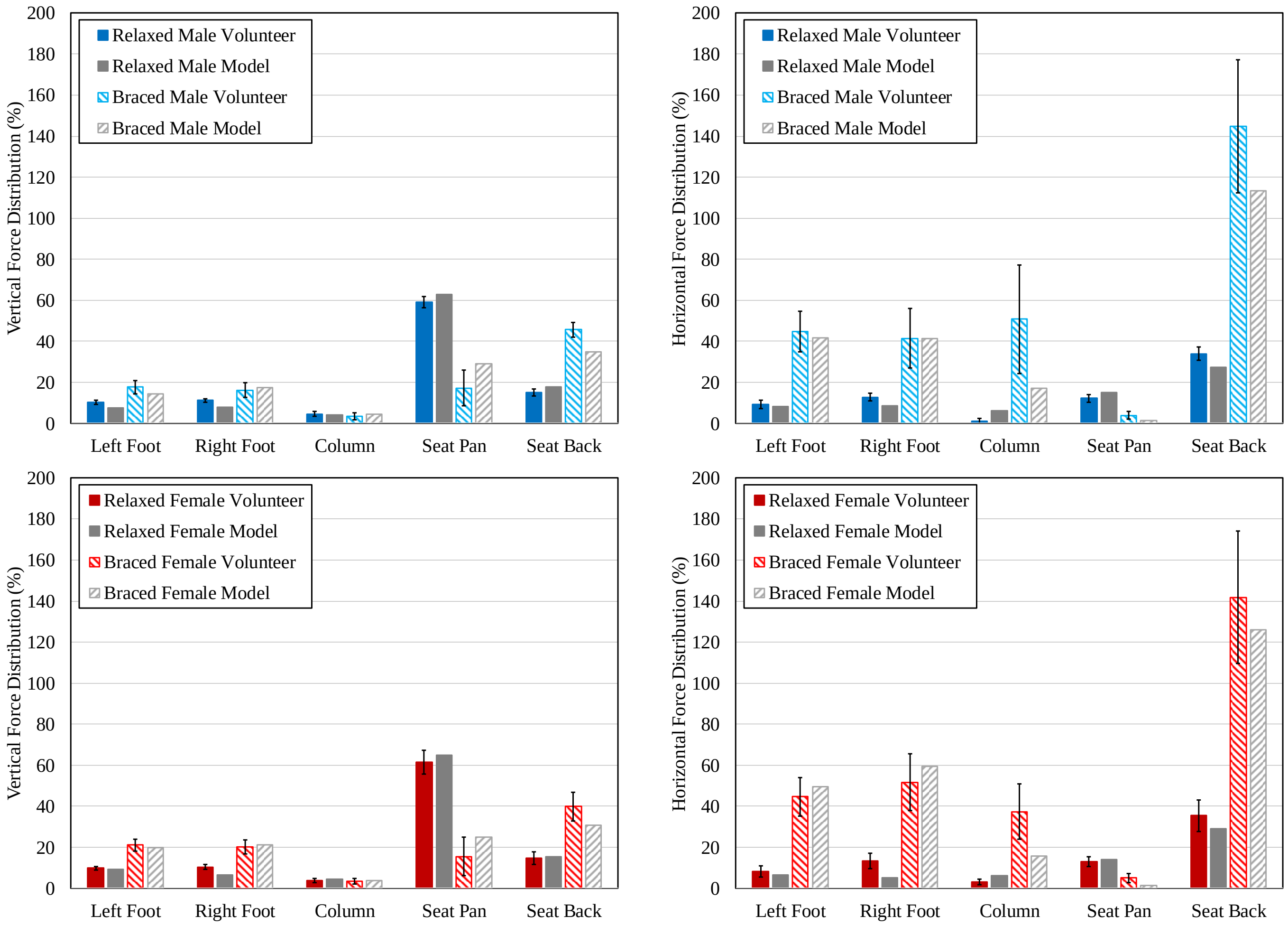

Fig. 11. Average vertical (left) and horizontal (right) force distributions for the male (top) and female (bottom) volunteers and models, for the relaxed (solid) and braced (striped) conditions. All percent force distributions are reported as absolute values.

TABLE VI

MODEL VERTICAL FORCE DISTRIBUTIONS (%)

	Sex	Left Foot	Right Foot	Column	Seat Pan	Seat Back
Relaxed	Female	9.1	6.3	4.5	64.9	15.3
	Male	7.6	7.8	4.0	63.0	17.7
Braced	Female	19.7	21.1	3.8	24.8	30.6
	Male	14.3	17.4	4.5	29.1	34.7

TABLE VII

VOLUNTEER VERTICAL FORCE DISTRIBUTIONS (%)

	Sex	Left Foot	Right Foot	Column	Seat Pan	Seat Back
Relaxed	Female	9.8 ± 0.8	10.3 ± 1.2	3.8 ± 0.9	61.5 ± 5.9	14.8 ± 3.1
	Male	10.2 ± 1.1	11.1 ± 0.8	4.6 ± 1.1	59.1 ± 2.7	14.9 ± 1.8
Braced	Female	21.1 ± 2.9	20.2 ± 3.4	3.4 ± 1.4	15.5 ± 9.3	39.9 ± 7.0
	Male	17.6 ± 3.2	16.2 ± 3.5	3.5 ± 1.7	17.1 ± 8.8	45.6 ± 3.7

TABLE VIII
MODEL HORIZONTAL FORCE DISTRIBUTIONS (%)

	Sex	Left Foot	Right Foot	Column	Seat Pan	Seat Back
Relaxed	Female	6.5	5.2	-6.2	14.1	-28.9
	Male	8.3	8.7	-6.2	15.1	-27.4
Braced	Female	49.4	59.3	15.6	1.5	-126.2
	Male	41.7	14.4	16.9	-1.2	-113.5

TABLE IX
VOLUNTEER HORIZONTAL FORCE DISTRIBUTIONS (%)

	Sex	Left Foot	Right Foot	Column	Seat Pan	Seat Back
Relaxed	Female	8.2 ± 2.8	13.3 ± 3.7	-3.2 ± 1.4	12.9 ± 2.4	-35.4 ± 7.7
	Male	9.3 ± 2.1	12.8 ± 2.0	-1.2 ± 1.3	12.2 ± 1.8	-34.0 ± 3.3
Braced	Female	44.6 ± 9.5	51.6 ± 13.8	37.4 ± 13.5	5.1 ± 2.2	-141.8 ± 32.3
	Male	44.8 ± 10.0	41.4 ± 14.4	50.7 ± 26.5	3.8 ± 1.8	-144.7 ± 32.4

TABLE X
MODEL RESULTANT FORCE DISTRIBUTIONS (%)

	Sex	Left Foot	Right Foot	Column	Seat Pan	Seat Back
Relaxed	Female	11.1	8.2	7.6	66.4	32.8
	Male	11.3	11.7	7.3	64.8	32.6
Braced	Female	53.3	63.0	16.0	24.9	129.9
	Male	44.1	44.9	17.5	29.1	118.7

TABLE XI
VOLUNTEER RESULTANT FORCE DISTRIBUTIONS (%)

	Sex	Left Foot	Right Foot	Column	Seat Pan	Seat Back
Relaxed	Female	12.9 ± 2.4	31.7 ± 2.5	4.0 ± 0.4	4.0 ± 0.4	236.8 ± 51.0
	Male	13.9 ± 2.2	46.5 ± 8.7	4.1 ± 1.5	4.1 ± 1.5	382.7 ± 138.0
Braced	Female	52.7 ± 9.8	58.9 ± 14.4	40.1 ± 14.3	17.8 ± 9.2	156.4 ± 34.0
	Male	51.0 ± 11.3	47.3 ± 15.7	54.4 ± 29.2	18.4 ± 8.9	160.7 ± 37.9

IV. DISCUSSION

Initial joint angles and force distributions were quantified and compared between relaxed and braced 5th percentile female and 50th percentile male volunteers to validate modifications to the test buck design. The initial joint angles and force distributions of the female volunteers were generally very similar to those of the male volunteers for each respective muscle condition, indicating that the test buck design successfully achieved similar initial conditions for both the 5th percentile female and 50th percentile male volunteers. Minimal differences in initial joint angles and force distributions were observed between the female and male volunteers in the braced condition, suggesting that initial conditions for this muscle condition may be slightly more variable compared to the relaxed condition. This could be attributed to a wide range of differences in bracing between individual subjects. For example, the observed 13° difference in elbow angle between the female and male volunteers when braced may be due to asymmetrical bracing observed in two female subjects. Compared to the other volunteers, these two subjects had noticeable visual differences in their left and right arms when bracing (i.e., straighter left arms). This could have resulted in bilateral differences in their elbow angles, which may explain the larger difference in elbow angle between sexes compared to other joint locations. However, unlike the relaxed condition, it was not necessarily expected that the initial joint angles and force distributions would match between sexes for the braced condition. The test buck modifications were designed such that the female and male volunteers' resting (relaxed) joint angles would be similar, but physical size differences between the sexes could reasonably explain potentially different initial joint angles and force distributions when braced.

Although examples of bracing variability were observed among the volunteers, in general bracing increased the volunteers' joint angles (as expected), particularly in the elbows. Across the vertical, horizontal, and resultant force distributions for the volunteers, bracing increased force distributions on the left and right foot pedals and seat back, but decreased force distributions on the seat pan. The increase in force distribution on the foot pedals and seat back was more prominent in the horizontal direction, and the decrease in force distribution on the seat pan was more prominent in the vertical direction. Bracing also increased the resultant force distribution on the steering column. Upon closer inspection, this increase in force distribution was primarily in the horizontal direction and not present in the vertical direction. These observations indicate that the volunteers braced as instructed, pushing their upper extremities, lower extremities, and torso toward the steering column, foot pedals, and seat back, respectively.

For the models, the initial joint angles and force distributions were also generally similar between females and males for each respective muscle condition. Similar to the volunteers, minimal differences in initial joint angles and and force distributions were observed in the braced condition compared to the relaxed condition. Bracing similarly increased the joint angles for the models, with the largest difference between muscle conditions being observed in the elbows. This likely indicates that both the volunteers' and models' upper bodies were translating the most in the sagittal plane when bracing, compared to their lower bodies. The trends observed in force distributions in the volunteers with respect to bracing were also generally present in the models.

Initial joint angles and force distributions were also quantified and compared between the volunteers and analogous models to determine if similar initial conditions were achieved in silico. Overall, the volunteers and models mostly had similar initial joint angles and force distributions for both sexes. The differences observed between the volunteers and models in initial joint angles and force distributions for the relaxed condition were minimal or negligible. However, some differences were observed between the volunteers and models when braced. Although the trends in force distributions for the volunteers on each of the reaction surfaces were captured by the models, it should be noted that the magnitude of the differences between muscle conditions was generally lower for the model. In particular, bracing increased the volunteer resultant force distributions on the steering column and seat back by 35-50% and 118-124%, respectively, but only increased the model resultant force distributions on the steering column and seat back by 8-10% and 86-97%, respectively. This could be attributed to a more prominent increase in the horizontal force distribution of braced volunteers compared to the braced models. The magnitude of the differences between muscle conditions was similar between the volunteers and models for the foot pedals and seat pan. These discrepancies in the magnitude of muscle condition differences on the reaction surfaces indicate that the models may not have captured the entire magnitude of bracing that the volunteers exerted on the test buck, particularly on the steering column and seat back. In general, the models may not have braced with as much upper body (steering column) and torso (seat back) force as the volunteers selected for this study.

The observed differences between the volunteers and models could be attributed to a number of factors. The initial joint angles for both the volunteers and models were calculated based on representative markers at specific anatomical locations. Efforts were made to match these locations between the volunteers and models as closely as possible. However, small discrepancies may still exist. For example, the locations of the motion capture markers used to calculate the head CG for the volunteers were determined visually using anatomical landmarks according to Table III, whereas the head CG for the models was calculated based on the mass distribution of the models' heads. For the force distributions, the observed differences between the volunteers and models when braced may be due to variations in anthropometry (e.g., height and weight) between the volunteers and models, or variations in other factors like muscle mass and size. A closer analysis of the force distributions for individual braced volunteers indicates that the braced models may have captured the magnitude of bracing for some, but not all, subjects. In particular, the braced models showed the least similarity to the volunteers in terms of force distributions on the steering column and seat back. For the same reaction surfaces, the volunteers showed the greatest inter-subject variability when braced. In fact, the models reasonably matched the steering column and seat back reaction forces during bracing for a subset of the volunteers who participated in this study. Another reason for bracing discrepancies may be the differences in feedback mechanisms used when bracing between the models and volunteers. The volunteers were able to initiate and adapt their bracing for two seconds prior to the test start in order to maximize force, as they were instructed to push with maximum effort, and ideally reach a steady state of bracing. However, the models used a closed-loop feedback control system for muscle activation that utilized joint angles as the control variables to adjust their bracing. It is notable that the force distributions differed between the braced volunteers and braced models despite similar initial joint angles. This demonstrates that both force distributions and initial positions should be considered when validating occupant models with active musculature.

The reported differences in initial joint angles and force distributions were important to quantify at the test start for several reasons. Comparing between sexes, the minimal differences in initial joint angles and force distributions helped validate the test buck design for the volunteers and indicated that similar initial conditions were achieved between sexes. This was necessary to consider because the test buck was modified for the 5th percentile female volunteers and confirming similar initial conditions between the female and male volunteers is a necessary requirement for making direct comparisons of dynamic occupant response data between volunteer groups in future work. Comparing between muscle conditions, the differences in initial joint angles and force distributions increased understanding of how pre-impact bracing could potentially change the initial state of an occupant during a pre-crash event or prior to a crash event. Finally, quantifying and comparing the initial joint angles and force distributions between the volunteers and models provided insight as to whether the models captured the initial conditions of the volunteers properly. Matching these initial conditions closely is imperative for the model to capture the occupant response accurately in a subsequent crash simulation.

Overall, the results from this study suggest that the computational HBMs with active musculature were capable of capturing the initial conditions observed in the female and male volunteers for both muscle conditions. However, the model more closely matched the initial conditions for the relaxed condition compared to the braced condition in terms of the magnitude of the reaction forces, particularly in the horizontal direction. This may be attributed to the difficulty in capturing the wide range of pre-impact bracing observed in the volunteers. The analysis presented here is limited due to the sample size of the volunteers. Recruiting and testing additional volunteers is necessary to more thoroughly understand differences in bracing variability and the frequency of certain anomalies, i.e., differences in bracing between the left and right side. Differences in how pre-test bracing affects volunteer and model kinematics and kinetics will be evaluated in future work.

V. CONCLUSIONS

The initial joint angles and reaction forces of small female and mid-size male volunteers and occupant models were quantified and compared to validate the test buck design and models. In general, the initial joint angles and vertical, horizontal, and resultant force distributions were similar between the volunteers and models, and between the female and male volunteers, for both relaxed and braced muscle conditions.

Differences in initial position and force distribution can affect occupant response during a subsequent MVC. It is therefore necessary, during model validation, for models to capture the initial conditions of volunteer data properly. However, these differences in initial conditions are not commonly reported in the model validation literature. This study provides novel volunteer data and the first in-depth validation of the initial joint angles and reaction forces of 5th percentile female and 50th percentile male computational HBMs with active musculature.

VI. ACKNOWLEDGEMENTS

The authors would like to thank the volunteers who participated in this study for their time and efforts, and the Global Human Body Models Consortium (Troy, MI, USA) for sponsoring this research.

VII. REFERENCES

[1] Devane, K., Johnson, D., and Gayzik, F.S. (2019) Validation of a simplified human body model in relaxed and braced conditions in low-speed frontal sled tests. Traffic Injury Prevention, **20**(8): p.832-837. https://doi.org/10.1080/15389588.2019.1655733.

[2] Iwamoto, M., Nakahira, Y., and Kimpara, H. (2015) Development and validation of the total human model for safety (THUMS) toward further understanding of occupant injury mechanisms in precrash and during crash. Traffic Injury Prevention, **16**(sup1): p.S36-S48. https://doi.org/10.1080/15389588.2015.1015000.

[3] Correia, M.A., McLachlin, S.D., and Cronin, D.S. (2020) Optimization of muscle activation schemes in a finite element neck model simulating volunteer frontal impact scenarios. Journal of Biomechanics, **104**: p.109754. https://doi.org/10.1016/j.jbiomech.2020.109754.

[4] Östh, J., Brolin, K., Carlsson, S., Wismans, J., and Davidsson, J. (2012) The occupant response to autonomous braking: a modeling approach that accounts for active musculature. Traffic Injury Prevention, **13**(3): p.265-277. https://doi.org/10.1080/15389588.2011.649437.

[5] Östh, J., Eliasson, E., Happee, R., and Brolin, K. (2014) A method to model anticipatory postural control in driver braking events. Gait & Posture, **40**(4): p.664-669. https://doi.org/10.1016/j.gaitpost.2014.07.021.

[6] Albert, D.L., Beeman, S.M., and Kemper, A.R. (2018) Occupant kinematics of the Hybrid III, THOR-M, and postmortem human surrogates under various restraint conditions in full-scale frontal sled tests. Traffic Injury Prevention, **19**(sup1): p.S50-S58. https://doi.org/10.1080/15389588.2017.1405390.

[7] Lopez-Valdes, F.J., Mroz, K., et al. (2018) Chest injuries of elderly postmortem human surrogates (PMHSs) under seat belt and airbag loading in frontal sled impacts: Comparison to matching THOR tests. Traffic Injury Prevention, **19**(sup2): p.S55-S63. https://doi.org/10.1080/15389588.2018.1542139.

[8] Beeman, S.M., Kemper, A.R., Madigan, M.L., and Duma, S.M. (2013) Kinetic and kinematic responses of post mortem human surrogates and the Hybrid III ATD in high-speed frontal sled tests. Accident Analysis & Prevention, **55**: p.34-47. https://doi.org/10.1016/j.aap.2013.02.015.

[9] Beeman, S.M., Kemper, A.R., Madigan, M.L., Franck, C.T., and Loftus, S.C. (2012) Occupant kinematics in low-speed frontal sled tests: Human volunteers, Hybrid III ATD, and PMHS. Accident Analysis & Prevention, **47**: p.128-139. https://doi.org/10.1016/j.aap.2012.01.016.

[10] Park, G., Kim, T., Crandall, J.R., Arregui Dalmases, C., and Luzón Narro, B.J. (2013) Comparison of kinematics of GHBMC to PMHS on the side impact condition. *Proceedings of the IRCOBI Europe Conference*, Gothenburg, Sweden. http://www.ircobi.org/wordpress/downloads/irc13/pdf_files/41.pdf.

[11] Arun, M.W., Umale, S., et al. (2016) Evaluation of kinematics and injuries to restrained occupants in far-side crashes using full-scale vehicle and human body models. Traffic Injury Prevention, **17**(sup1): p.116-123. https://doi.org/10.1080/15389588.2016.1197394.

[12] Katagiri, M., Zhao, J., Kerrigan, J., Kent, R., and Forman, J. (2016) Comparison of whole-body kinematic behaviour of the GHBMC occupant model to PMHS in far-side sled tests. *Proceedings of the IRCOBI Europe Conference*, Malaga, Spain. http://www.ircobi.org/wordpress/downloads/irc16/pdf-files/88.pdf.

[13] Katagiri, M., Zhao, J., Lee, S., Moorhouse, K., and Kang, Y.-S. (2019) Biofidelity evaluation of GHBMC male occupant models in rear impacts. *Proceedings of the IRCOBI Europe Conference*, Florence, Italy. http://www.ircobi.org/wordpress/downloads/irc19/pdf-files/52.pdf.

[14] Hwang, E., Hu, J., and Reed, M.P. (2020) Validating diverse human body models against side impact tests with post-mortem human subjects. Journal of Biomechanics, **98**: p.109444. https://doi.org/10.1016/j.jbiomech.2019.109444.

[15] Poulard, D., Subit, D., Nie, B., Donlon, J.-P., and Kent, R.W. (2015) The contribution of pre-impact posture on restrained occupant finite element model response in frontal impact. Traffic Injury Prevention, **16**(sup2): p.S87-S95. https://doi.org/10.1080/15389588.2015.1064529.

[16] Bose, D., Crandall, J., Untaroiu, C., and Maslen, E. (2008) Influence of pre-collision occupant properties on the injury response during frontal collision. *Proceedings of the IRCOBI Europe Conference*, Bern, Switzerland. http://www.ircobi.org/wordpress/downloads/irc0111/2008/Session3/3_1.pdf.

[17] Ando, T., Kitagawa, Y., and Eggers, A. (2019) Influence of posture adjustment methods for human body models on injury prediction. *Proceedings of the IRCOBI Europe Conference*, Florence, Italy. http://www.ircobi.org/wordpress/downloads/irc19/pdf-files/56.pdf.

[18] Schap, J.M., Koya, B., and Gayzik, F.S. (2019) Objective evaluation of whole body kinematics in a simulated, restrained frontal impact. Annals of Biomedical Engineering, **47**(2): p.512-523. https://doi.org/10.1007/s10439-018-02180-2.
[19] Vavalle, N.A., Thompson, A.B., et al. (2014) Investigation of the mass distribution of a detailed seated male finite element model. Journal of Applied Biomechanics, **30**(3): p.471-476. https://doi.org/10.1123/jab.2013-0007.
[20] Thompson, A.B., Rhyne, A.C., Moreno, D.P., Gayzik, F.S., and Stitzel, J.D. (2011) Methods for validation of the mass distribution of a full body finite element model-biomed 2011. Biomedical Sciences Instrumentation, **47**: p.100-105. PMID: 21525604.
[21] Bose, D., Crandall, J.R., Untaroiu, C.D., and Maslen, E. (2010) Influence of pre-collision occupant parameters on injury outcome in a frontal collision. Accident Analysis & Prevention, **42**(4): p.1398-1407. https://doi.org/10.1016/j.aap.2010.03.004.
[22] Chan, H., Albert, D.L., Gayzik, F.S., and Kemper, A.R. (2021) Assessment of acclimation of 5th percentile female and 50th male volunteer kinematics in low-speed frontal and frontal-oblique sled tests. SAE International Journal of Transportation Safety, **9**(1): p.3-103.
[23] Schneider, L.W., Robbins, D.H., Pflüg, M.A., and Snyder, R.G., (1983) NHTSA, *Development of anthropometrically based design specifications for an advanced adult anthropomorphic dummy family, volume 1*, US Department of Transportation, Washington, DC.
[24] Beeman, S.M., Kemper, A.R., Madigan, M.L., and Duma, S.M. (2011) Effects of bracing on human kinematics in low-speed frontal sled tests. Annals of Biomedical Engineering, **39**(12): p.2998. https://doi.org/10.1007/s10439-011-0379-1.
[25] Vital, J. and Senegas, J. (1986) Anatomical bases of the study of the constraints to which the cervical spine is subject in the sagittal plane: A study of the center of gravity of the head. Surgical and Radiologic Anatomy, **8**(3): p.169-173. https://doi.org/10.1007/bf02427845.
[26] Walker, L.B., Harris, E.H., and Pontius, U.R. Mass, volume, center of mass, and mass moment of inertia of head and head and neck of human body. https://doi.org/10.4271/730985.
[27] SAE. Instrumentation for impact test—Part 1—Electronic instrumentation. 2014.

VIII. APPENDIX

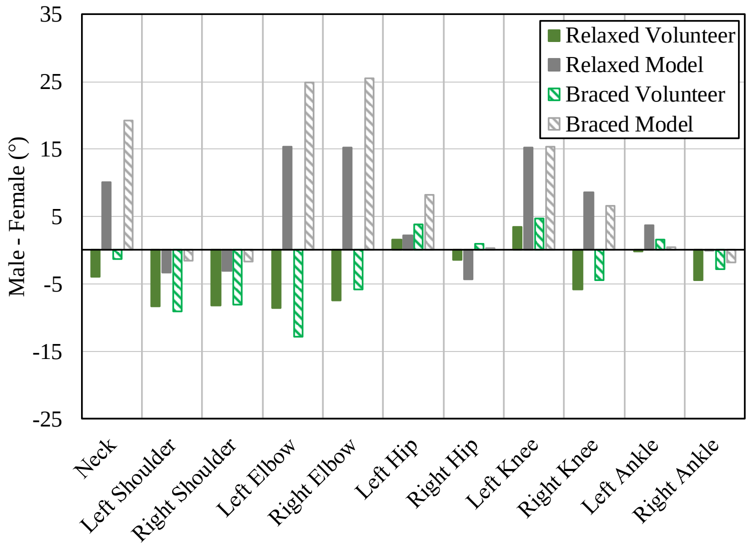

Fig. A1. Joint angle comparisons between sexes (male – female).

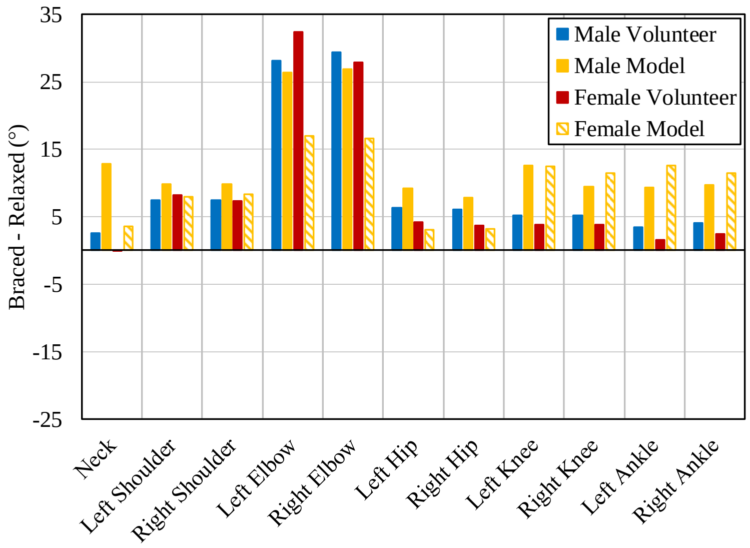

Fig. A2. Joint angle comparisons between muscle conditions (braced – relaxed).

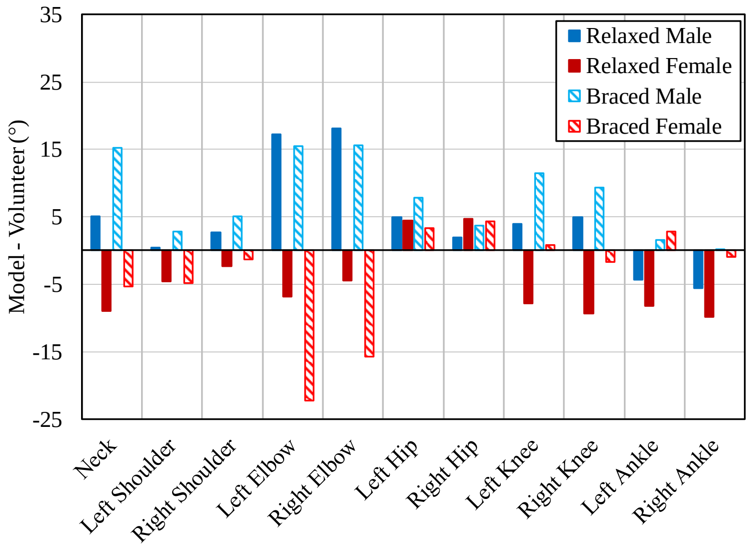

Fig. A3. Joint angle comparisons between the volunteers and models (model – volunteer).

TABLE A I

JOINT ANGLE DIFFERENCES: MALE - FEMALE (°)

	Relaxed		Braced	
	Volunteer	Model	Volunteer	Model
Neck	-4	10	-1	19
Left shoulder	-8	-3	-9	-2
Right shoulder	-8	-3	-8	-2
Left elbow	-9	15	-13	25
Right elbow	-7	15	-6	25
Left hip	2	2	4	8
Right hip	-5	-4	1	0
Left knee	3	15	5	15
Right knee	-6	9	-4	7
Left ankle	0	4	2	0
Right ankle	-4	0	-3	-2

TABLE A II

JOINT ANGLE DIFFERENCES: BRACED - RELAXED (°)

	Male		Female	
	Volunteer	Model	Volunteer	Model
Neck	3	13	0	4
Left shoulder	7	10	8	8
Right shoulder	7	10	7	8
Left elbow	28	26	32	17
Right elbow	29	27	28	17
Left hip	6	9	4	3
Right hip	6	8	4	3
Left knee	5	13	4	13
Right knee	5	9	4	11
Left ankle	3	9	2	13
Right ankle	4	10	2	11

TABLE A III

JOINT ANGLE DIFFERENCES: MODEL – VOLUNTEER (°)

	Relaxed		Braced	
	Female	Male	Female	Male
Neck	-9	5	-5	15
Left shoulder	-5	0	-5	3
Right shoulder	-2	3	-1	5
Left elbow	-7	17	-22	16
Right elbow	-5	18	-16	16
Left hip	4	5	3	8
Right hip	5	2	4	4
Left knee	-8	4	1	11
Right knee	-9	5	-2	9
Left ankle	-8	-4	3	2
Right ankle	-10	-6	-1	0

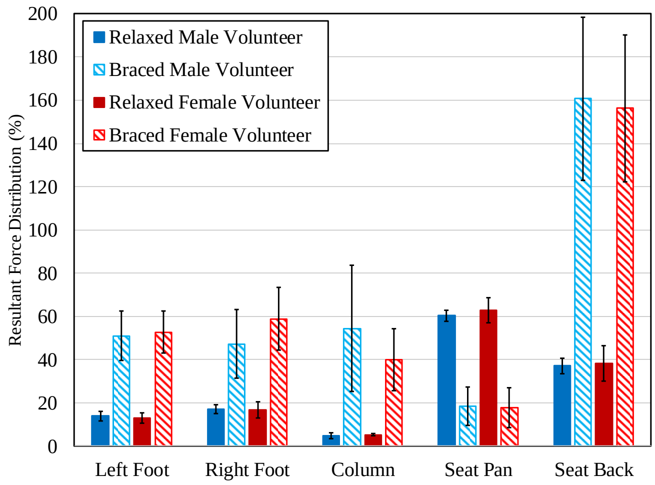

Fig. A4. Average resultant force distributions for the male (blue) and female (red) volunteer for the relaxed (solid) and braced (striped) conditions. All percent force distributions are reported as absolute values.

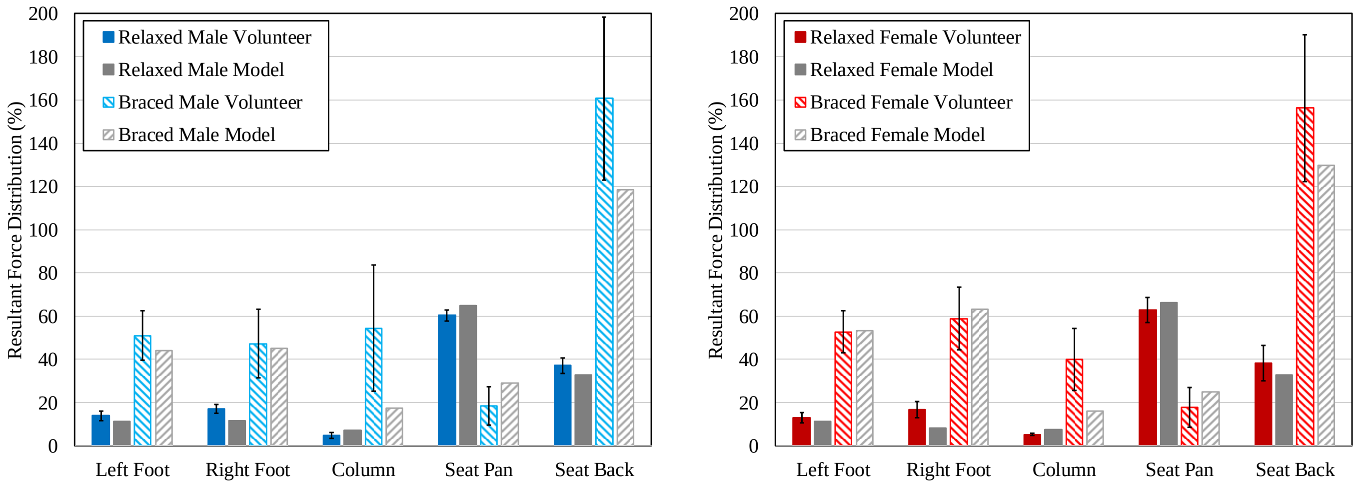

Fig. A5. Average resultant force distributions for the male volunteers (left, blue) and male models (left, grey), and the female volunteers (right, red) and female models (right, grey), for the relaxed (solid) and braced (striped) conditions. All percent force distributions are reported as absolute values.

TABLE A IV

MODEL VERTICAL FORCE DISTRIBUTIONS (N)

	Sex	Left Foot	Right Foot	Column	Seat Pan	Seat Back
Relaxed	Female	44.0	30.7	21.8	315.8	74.4
	Male	56.4	58.1	29.6	470.3	132.1
Braced	Female	107.5	115.4	20.9	135.6	167.0
	Male	123.9	150.9	38.9	251.4	300.6

TABLE A V

VOLUNTEER VERTICAL FORCE DISTRIBUTIONS (N)

	Sex	Left Foot	Right Foot	Column	Seat Pan	Seat Back
Relaxed	Female	47.4 ± 5.2	49.8 ± 7.1	18.4 ± 4.7	297.8 ± 29.6	71.8 ± 16.2
	Male	75.3 ± 8.1	81.9 ± 5.0	33.8 ± 9.1	435.5 ± 25.8	110.0 ± 14.6
Braced	Female	108.2 ± 15.5	104.1 ± 21.0	17.6 ± 7.5	78.7 ± 45.0	205.7 ± 41.2
	Male	136.7 ± 24.5	125.7 ± 28.8	26.7 ± 13.2	132.7 ± 67.7	353.4 ± 29.5

TABLE A VI

MODEL HORIZONTAL FORCE DISTRIBUTIONS (N)

	Sex	Left Foot	Right Foot	Column	Seat Pan	Seat Back
Relaxed	Female	31.5	25.2	-30.1	68.4	-140.8
	Male	62.2	64.8	-45.9	112.6	-204.3
Braced	Female	270.1	324.1	85.0	8.1	-689.5
	Male	360.9	358.5	146.3	-10.6	-982.1

TABLE A VII

VOLUNTEER HORIZONTAL FORCE DISTRIBUTIONS (N)

	Sex	Left Foot	Right Foot	Column	Seat Pan	Seat Back
Relaxed	Female	39.6 ± 13.7	64.3 ± 18.3	-15.4 ± 7.1	62.6 ± 13.1	-171.7 ± 39.3
	Male	68.2 ± 14.0	94.0 ± 13.7	-8.7 ± 10.2	89.9 ± 16.7	-250.0 ± 25.4
Braced	Female	229.6 ± 51.4	267.2 ± 82.9	193.6 ± 75.4	26.2 ± 11.4	-732.7 ± 193.5
	Male	346.8 ± 77.7	322.4 ± 114.9	390.0 ± 200.5	29.8 ± 14.1	-1120.3 ± 246.1

TABLE A VIII

MODEL RESULTANT FORCE DISTRIBUTIONS (N)

	Sex	Left Foot	Right Foot	Column	Seat Pan	Seat Back
Relaxed	Female	54.1	39.7	37.2	323.1	159.4
	Male	84.0	87.2	54.6	483.6	243.6
Braced	Female	291.2	344.3	87.6	135.9	709.5
	Male	381.6	389.0	151.8	251.7	1027.1

TABLE A IX

VOLUNTEER RESULTANT FORCE DISTRIBUTIONS (N)

	Sex	Left Foot	Right Foot	Column	Seat Pan	Seat Back
Relaxed	Female	62.6 ± 12.0	81.5 ± 18.5	25.0 ± 3.2	304.4 ± 29.7	186.2 ± 42.2
	Male	102.0 ± 14.9	124.8 ± 13.4	35.8 ± 10.8	444.7 ± 27.1	273.2 ± 28.3
Braced	Female	255.5 ± 48.8	287.7 ± 85.1	195.6 ± 75.3	85.9 ± 42.8	762.1 ± 195.7
	Male	374.3 ± 76.3	349.0 ± 116.4	393.1 ± 198.3	137.0 ± 67.8	1176.9 ± 242.7

TABLE A X

VERTICAL FORCE DISTRIBUTION DIFFERENCES: MALE - FEMALE (%)

	Relaxed		Braced	
	Volunteer	Model	Volunteer	Model
Left foot	0	-1	-3	-5
Right foot	1	1	-4	-4
Column	1	-1	0	1
Seat Pan	-2	-2	2	4
Seat Back	0	2	6	4

TABLE A XI

HORIZONTAL FORCE DISTRIBUTION DIFFERENCES: MALE - FEMALE (%)

	Relaxed		Braced	
	Volunteer	Model	Volunteer	Model
Left foot	1	2	0	-8
Right foot	0	4	-10	-18
Column	2	0	13	1
Seat Pan	-1	1	-1	-3
Seat Back	1	2	-3	13

TABLE A XII

RESULTANT FORCE DISTRIBUTION DIFFERENCES: MALE - FEMALE (%)

	Relaxed		Braced	
	Volunteer	Model	Volunteer	Model
Left foot	1	0	-2	-9
Right foot	0	4	-12	-18
Column	0	0	14	2
Seat Pan	-2	-2	1	4
Seat Back	-1	0	4	-11

TABLE A XIII

VERTICAL FORCE DISTRIBUTION DIFFERENCES: BRACED - RELAXED (%)

	Male		Female	
	Volunteer	Model	Volunteer	Model
Left foot	7	7	11	11
Right foot	5	10	10	15
Column	-1	1	0	-1
Seat Pan	-42	-34	-46	-40
Seat Back	31	17	25	15

TABLE A XIV

HORIZONTAL FORCE DISTRIBUTION DIFFERENCES: BRACED - RELAXED (%)

	Male		Female	
	Volunteer	Model	Volunteer	Model
Left foot	35	33	36	43
Right foot	29	33	38	54
Column	42	23	41	22
Seat Pan	-8	-16	-8	-13
Seat Back	-111	-86	-106	-97

TABLE A XV

RESULTANT FORCE DISTRIBUTION DIFFERENCES: BRACED - RELAXED (%)

	Male		Female	
	Volunteer	Model	Volunteer	Model
Left foot	37	33	40	42
Right foot	30	33	42	55
Column	50	10	35	8
Seat Pan	-42	-36	-45	-42
Seat Back	124	86	118	97

TABLE A XVI

VERTICAL FORCE DISTRIBUTION DIFFERENCES: MODEL - VOLUNTEER (%)

	Relaxed		Braced	
	Female	Male	Female	Male
Left foot	-1	-3	-1	-3
Right foot	-4	-3	1	1
Column	1	-1	0	1
Seat Pan	3	4	9	12
Seat Back	1	3	-9	-11

TABLE A XVII

HORIZONTAL FORCE DISTRIBUTION DIFFERENCES: MODEL - VOLUNTEER (%)

	Relaxed		Braced	
	Female	Male	Female	Male
Left foot	-2	-1	5	-3
Right foot	-8	-4	8	0
Column	-3	-5	-22	-34
Seat Pan	1	3	-4	-6
Seat Back	6	7	16	31

TABLE A XVIII

RESULTANT FORCE DISTRIBUTION DIFFERENCES: MODEL - VOLUNTEER (%)

	Relaxed		Braced	
	Female	Male	Female	Male
Left foot	-2	-3	1	-7
Right foot	-9	-5	4	-2
Column	2	2	-24	-37
Seat Pan	4	4	7	11
Seat Back	-6	-4	-27	-42

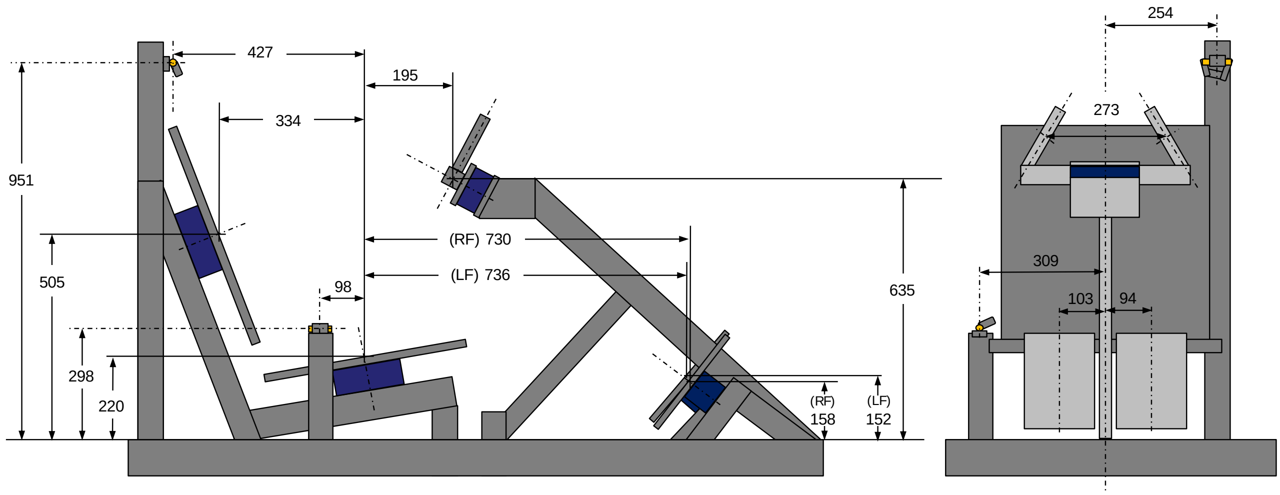

Fig. A6. Test buck dimensions (mm) for the 50th percentile male volunteers. Measurements were obtained using a portable coordinate measuring machine with a point probe (8 ft-7 axis Platinum FaroArm, FARO Technologies, Inc., Lake Mary, FL, USA).

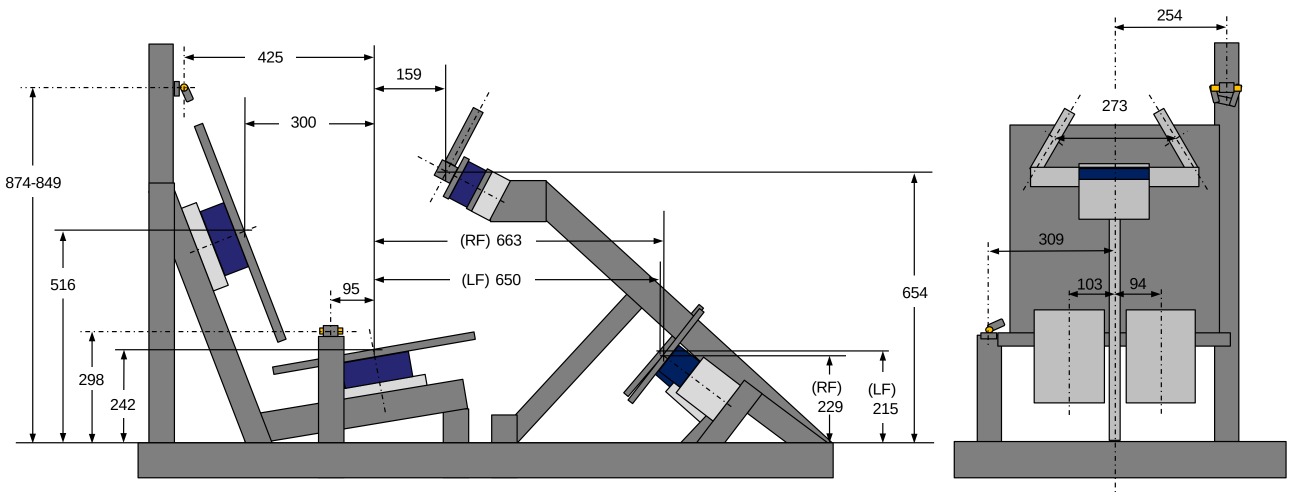

Fig. A7. Test buck dimensions (mm) for the 5th percentile female volunteers. Measurements were obtained using a portable coordinate measuring machine with a point probe (8 ft-7 axis Platinum FaroArm).